

The Accurate Particle Tracer Code

Yulei Wang^a, Jian Liu^{a,*}, Hong Qin^{a,b}, Zhi Yu^c, Yicun Yao^a

^a*School of Nuclear Science and Technology and Department of Modern Physics, University of Science and Technology of China, Hefei, Anhui 230026, China*

^b*Plasma Physics Laboratory, Princeton University, Princeton, NJ 08543, USA*

^c*Theory and Simulation Division, Institute of Plasma Physics, Chinese Academy of Sciences, Hefei, Anhui 230031, China*

Abstract

The Accurate Particle Tracer (APT) code is designed for systematic large-scale applications of geometric algorithms for particle dynamical simulations. Based on a large variety of advanced geometric algorithms, APT possesses long-term numerical accuracy and stability, which are critical for solving multi-scale and nonlinear problems. To provide a flexible and convenient I/O interface, the libraries of Lua and Hdf5 are used. Following a three-step procedure, users can efficiently extend the libraries of electromagnetic configurations, external non-electromagnetic forces, particle pushers, and initialization approaches by use of the extendible module. APT has been used in simulations of key physical problems, such as runaway electrons in tokamaks and energetic particles in Van Allen belt. As an important realization, the APT-SW version has been successfully distributed on the world's fastest computer, the Sunway TaihuLight supercomputer, by supporting master-slave architecture of Sunway many-core processors. Based on large-scale simulations of a runaway beam under parameters of the ITER tokamak, it is revealed that the magnetic ripple field can disperse the pitch-angle distribution significantly and improve the confinement of energetic runaway beam on the same time.

Keywords: Structure-Preserving Algorithms, Plasma simulation, Multi-timescale Dynamics, Large-scale Simulation

*Corresponding author

Email address: jliuphy@ustc.edu.cn (Jian Liu)

1. Introduction

Nonlinear and multi-scale dynamical processes are ubiquitous in different fields of scientific and engineering researches. Especially in plasma physics, where long-range collective phenomena dominate, advanced numerical schemes and powerful computing software are required for solving complex physical and technical problems. The GeoAlgorithmic Plasma Simulator (GAPS) project is initiated in order to solve various difficult yet key problems in plasma-related domains by applying advanced geometric algorithms and modern large-scale simulation techniques. The Accurate Particle Tracer (APT) code is one product of the GAPS project and aims to facilitate the systematic large-scale applications of advanced algorithms for particle dynamical simulations.

Particle dynamical simulations play important roles in numerical studies of plasmas. Various codes have been developed and used widely for solving problems including the particle acceleration in magnetic reconnection [1, 2], fast particle dynamics in Tokamaks [3, 4], wave-particle interactions in earth magnetosphere [5], and particle transportation in plasma turbulences [6, 7]. The particle dynamical simulation is also a main method of solving differential stochastic equations, when stochastic processes of plasmas are considered, such as the simulation of runaway dynamics during disruptions of tokamak operations [8].

Although fruitful results have been achieved, the accumulation of numerical errors makes traditional codes unreliable after long-term simulations which are unavoidable for addressing multi-scale and nonlinear problems. Real physical information may also be distorted due to the breakdown of original physical structures in computation schemes. To guarantee long-term numerical accuracy and stability, a series of advanced geometric algorithms have been systematically developed recently [9–34], which bound the global numerical errors by preserving geometric structures. On the other hand, the further development and application of geometric algorithms needs interdisciplinary cooperation. An

efficient platform for researchers in different fields is needed to integrate the latest trans-disciplinary achievements.

In this paper, we introduce the design details, numerical strategies, use instructions, and novel physical results of the APT code. Different from the particle dynamical codes equipped with traditional algorithms and focusing only on some specific physical application scenarios [1–3, 6, 7], the APT code is based on geometric algorithms with secular stability, and its algorithm and physical libraries can also be extended conveniently to accomplish tasks in various research fields. Therefore, APT not only can be used to address multi-scale and nonlinear problems, but also serves as a universal platform for researchers from different fields, such as plasma physics, accelerator physics, space science, fusion energy research, computational mathematics, software engineering, and high-performance computation.

The underlying model of APT is the first principle particle dynamical equations. In simulations of plasma systems, the distribution of plasmas is sampled statistically in the phase space. Using appropriate geometric algorithms, APT traces each sample point accurately by solving full-orbit Lorentz force equations that are the characteristic line equations of the Vlasov equation. If considering the random collisional terms, the Langevin approach is used, which transfers the collisional terms to random forces [35]. The external electromagnetic fields are set up through analytical functions, or discrete field configuration data obtained from experiments or simulations. There already exist many built-in electromagnetic field configurations for typical physical problems in APT. Self-consistent calculation of APT is implemented through dynamical field models, namely, field functions with variable parameters evolving together with the phase-space states of all particles.

The APT code is implemented in standard C language and can be distributed directly on Unix-like operation system. For non-Unix-like systems, users can build APT via Unix-like compatibility layers, such as Cygwin and MSYS. The APT code consists of seven main modules, including the I/O module, the initialization module, the particle pusher module, the parallelization module, the

field configuration module, the external force-field module, and the extendible module. The I/O module calls the libraries from Lua and Hdf5 projects. The input configuration files consist of several Lua scripts which make it convenient and flexible for users to set the parameters of physical problems. The output data is stored in the Hdf5 format, which enables users to access data in a file-system-like way and simplifies data analysis. The initialization module provides a number of methods for statistical sampling. The particle pusher module contains various advanced geometric algorithms, including volume-preserving and symplectic integrators with different orders and stability domains. Traditional algorithms such as Runge-Kutta method with different orders are also available. It is thus convenient to choose appropriate algorithms for solving realistic problems and studying numerical methods under complex physical setup. To boost large-scale applications of geometric algorithms, the parallelization module of the stable APT distribution supports the MPI parallelization. Another version of APT supporting CUDA is also developed. As an important parallel version, the branch version APT-SW has been built recently for the world's fastest supercomputer, the Sunway TaihuLight supercomputer [36], which provides more than ten million computation cores and has the peak performance of 125PFlops [37]. To fully utilize the computation ability of the Sunway TaihuLight, APT-SW is designed to support the Sunway many-core parallelization. Supported by the powerful computation capacity, APT-SW can be used to simulate processes with large amounts of sampling particles, complex field configurations, and multi-timescales spanning more than 10 orders. The field configuration module and the external force-field module contain respectively various electromagnetic configurations and other external non-electromagnetic force fields, such as radiation force, collisional force, bremsstrahlung force, and gravitation field. Written by the bash-script, the extendible module provides a convenient way to extend the source code. Following the interfaces of APT and a three-step extending procedure, one can easily add new configuration parameters, field configurations, external forces, algorithms, and initialization functions into APT. These new packages form a new version of APT, and can also be used

by other researchers. The detailed introductions about the interfaces and the procedure to use and extend APT are provided in this paper.

APT has been used in the study of geometric numerical methods and the simulations of some multi-scale physical processes [38, 39]. In this paper, we present two benchmarks from plasma physics. In the first case, the multi-scale dynamics of runaway electrons in tokamaks is studied by secular simulations over 10^{12} time steps. Using the relativistic volume-preserving algorithm in APT, the refined structures of runaway transit orbits are revealed. The APT code shows long-term numerical accuracy and enables the discovery of novel mechanisms such as neoclassical collisionless pitch-angle scattering and new runaway energy limit rule [38, 39]. In the second case, the evolution of energetic particle distribution in Van Allen belt is simulated by tracing massive sampling particles. The symplectic Euler pusher for relativistic dynamics is employed. The evolution of energetic particles in the terrestrial magnetic field is recovered precisely.

New physical results have been obtained based on the large-scale simulations of APT-SW. The long-term evolution of the runaway electron beam under the realistic parameters of ITER tokamak is simulated on the TaihuLight supercomputer. This simulation involves approximately 10^7 samplings, 10^{11} iteration steps, and more than 10^{21} floating-point operations, which is currently the largest particle simulation. Both the neoclassical collisionless pitch-angle scattering [38] and the magnetic ripple stochastic effect are considered [39, 40]. Without magnetic ripple field, after long-term evolution, the pitch-angle distribution tends to be concentrated in a small interval and has non-zero average value, which is consistent with the results in Ref. [39]. However, if the magnetic ripple is considered, the pitch-angle distribution can be significantly dispersed. Meanwhile, the poloidal profile of runaway beam is proven to be squeezed towards tokamak core by the magnetic ripple field, which serves as an evidence to the improved confinement of runaway electrons.

The remaining part of the paper is organized as follows. The introductions on APT, including the numerical strategy, the parallelization methods, and the procedures of using and extending APT, are provided in Sec. 2. In Sec. 3, two

typical benchmarks under different physical backgrounds carried out by APT are exhibited. The novel physical results of large-scale simulation of runaway electrons on the Sunway TaihuLight supercomputer are discussed in Sec. 4. Section 5 gives a brief summary.

2. Architecture of Apt

As a product of the GAPS project, APT aims to benefit simulations of various research fields through the long-term accuracy of geometric algorithms. In order to accelerate the development and optimization of geometric algorithms, and form a convenient platform for integrating novel techniques from different fields, the architecture of APT is designed to be modularized and extendible. Figure 1 depicts the design schematic of the APT code. There are five containers for configuration parameters, electromagnetic functions, external forces, particle pushers, and initialization methods. Besides using the functions already integrated in APT, one can also conveniently add new variables, electromagnetic field configurations, external forces, algorithms as well as initialization approaches into these containers through the extendible module, see the brown arrows in Fig. 1. The built-in geometric algorithms in the pusher container provide the APT code with secular stability and accuracy. As is shown by the blue arrows in Fig. 1, users can set all configuration parameters required by a specific task in one Lua configuration file, which loads appropriate values into the parameter container. Then, these parameters control APT to load selected modules from corresponding containers, and manage the processes of parallelization, iteration, and data output. In this section, we introduce the numerical strategy and the parallelization implementations of APT. Meanwhile, we exhibit the detailed procedures of installing, using, and extending APT.

2.1. The numerical strategy of APT

The fundamental numerical method of the APT code is based on the first principle particle dynamical equations. The evolution of every particle is gov-

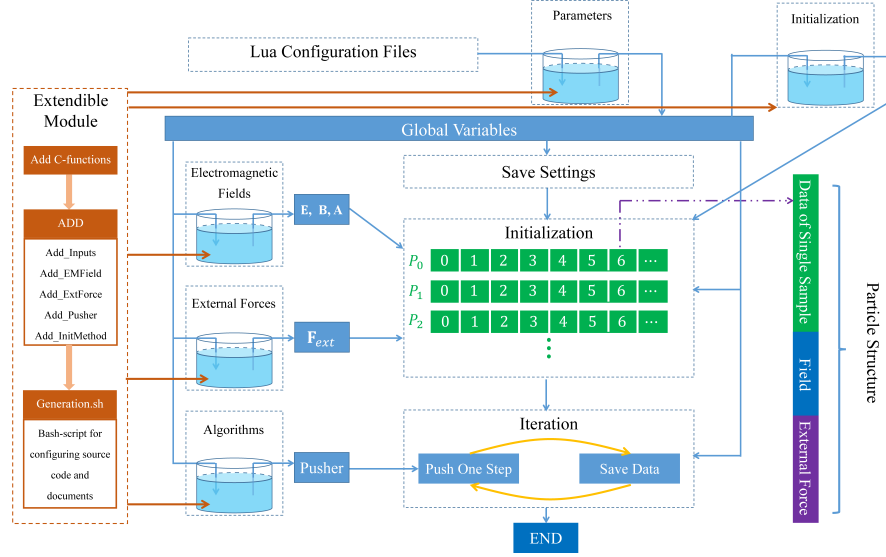


Figure 1: Diagram of the APT architecture. The blue arrows denote the flow of procedure, while the brown parts represent the extendible module. In the Initialization box, sampling particles assigned to different processors are marked by P_0, P_1, P_2, \dots .

erned by both the electromagnetic force (the Lorentz force) and external non-electromagnetic forces. When dealing with the electromagnetic forces, APT uses structure-preserving geometric algorithms to ensure the secular numerical stability. Because the design of APT aims to form a platform for studying and using geometric algorithms, there is more than one geometric pusher integrated in the particle pusher module. If more users join the APT project and extend the libraries, more algorithms will be included. So, it is not possible and not necessary to present the details of all built-in algorithms. However, it is still helpful to exhibit two typical algorithms to clarify the framework of numerical strategy used in APT.

The first example is the volume-preserving algorithm (VPA) for relativistic

charged particles, which solves directly the Newton motion equation, namely,

$$\frac{d\mathbf{x}}{dt} = \frac{\mathbf{p}}{m\gamma}, \quad (1)$$

$$\frac{d\mathbf{p}}{dt} = q \left(\mathbf{E} + \frac{\mathbf{p} \times \mathbf{B}}{m\gamma} \right), \quad (2)$$

where \mathbf{x} and \mathbf{p} denote respectively position and momentum, γ is the Lorentz factor, m is rest mass of a particle, q is the particle charge, and \mathbf{E} and \mathbf{B} denote electric field and magnetic field, respectively. Various kinds of VPAs have been established in different ways [13, 15, 19, 20]. For example, the discrete equations of a 2-order VPA integrated in APT is

$$\mathbf{x}_{k+\frac{1}{2}} = \mathbf{x}_k + \frac{\Delta t}{2} \frac{\mathbf{p}_k}{\sqrt{m^2 + \mathbf{p}_k^2/c^2}}, \quad (3)$$

$$\mathbf{p}^- = \mathbf{p}_k + \frac{\Delta t}{2} \left(q\mathbf{E}_{k+\frac{1}{2}} \right), \quad (4)$$

$$\mathbf{p}^+ = \text{Cay} \left(\frac{q\Delta t \hat{\mathbf{B}}_{k+1/2}}{2\sqrt{m^2 + (\mathbf{p}^-)^2/c^2}} \right) \mathbf{p}^-, \quad (5)$$

$$\mathbf{p}_{k+1} = \mathbf{p}^+ + \frac{\Delta t}{2} \left(q\mathbf{E}_{k+\frac{1}{2}} \right), \quad (6)$$

$$\mathbf{x}_k = \mathbf{x}_{k+\frac{1}{2}} + \frac{\Delta t}{2} \frac{\mathbf{p}_{k+1}}{\sqrt{m^2 + \mathbf{p}_{k+1}^2/c^2}}, \quad (7)$$

where the subscript, k , denotes the k -th step, Δt is the time step length, $\hat{\mathbf{B}}$ is defined as

$$\hat{\mathbf{B}} = \begin{pmatrix} 0 & B_z & -B_y \\ -B_z & 0 & B_x \\ B_y & -B_x & 0 \end{pmatrix}, \quad (8)$$

and the symbol Cay denotes the Cayley transform [15]. Another example is 1-order canonical symplectic Euler algorithm for relativistic particles, which discretizes the Hamiltonian equation,

$$\frac{d\mathbf{P}}{dt} = -\frac{\partial H}{\partial \mathbf{X}}, \quad \frac{d\mathbf{X}}{dt} = -\frac{\partial H}{\partial \mathbf{P}}, \quad (9)$$

where, \mathbf{P} and \mathbf{X} are respectively canonical momentum and canonical coordinate, \mathbf{A} denotes the vector potential, ϕ is the scalar potential, and the Hamiltonian

is $H(\mathbf{P}, \mathbf{X}) = \sqrt{[\mathbf{P} - q\mathbf{A}(\mathbf{X})]^2 c^2 + m^2 c^4} + q\phi$. The corresponding canonical symplectic Euler algorithm is

$$\mathbf{P}_{k+1} = \mathbf{P}_k - \Delta t \left[-\frac{q(\mathbf{P}_{k+1} - q\mathbf{A}_k) \cdot \nabla \mathbf{A}_k}{m\gamma(\mathbf{P}_{k+1}, \mathbf{X}_k)} + q\nabla\phi_k \right], \quad (10)$$

$$\mathbf{X}_{k+1} = \mathbf{X}_k + \Delta t \left[\frac{\mathbf{P}_{k+1} - q\mathbf{A}_k}{m\gamma(\mathbf{P}_{k+1}, \mathbf{X}_k)} \right]. \quad (11)$$

For charged particle systems with electromagnetic forces, the geometric structures and corresponding structure-preserving algorithms have been studied in detail. Fruitful results have been published on this topic. However, in many situations, physical systems can be very complex, and involve many non-electromagnetic forces. Some of these forces possess clear mathematical structures, such as gravitational force, while some don't, such as radiation force of charged particles. When dealing with external non-electromagnetic forces, for geometric algorithms based on Newton equations like Eqs. 3-7, the basic idea of APT is to separate the calculations of electromagnetic and non-electromagnetic forces. For the default calculation mode, the electromagnetic forces of motion equation are calculated by structure-preserving algorithms, while the non-electromagnetic forces, \mathbf{F}_{ext} , are treated as effective electric fields within the discrete one-step map. To be specific, after including the external force terms, Eq. 4 and Eq. 6 become

$$\mathbf{p}^- = \mathbf{p}_k + \frac{\Delta t}{2} \left(q\mathbf{E}_{k+\frac{1}{2}} + \mathbf{F}_{ext, k+\frac{1}{2}} \right), \quad (12)$$

$$\mathbf{p}_{k+1} = \mathbf{p}^+ + \frac{\Delta t}{2} \left(q\mathbf{E}_{k+\frac{1}{2}} + \mathbf{F}_{ext, k+\frac{1}{2}} \right). \quad (13)$$

Generally speaking, the external forces can be functions of arbitrary order derivatives of \mathbf{x} , namely, $\mathbf{F}_{ext} = \mathbf{F}_{ext}(\mathbf{x}, \dot{\mathbf{x}}, \ddot{\mathbf{x}}, \dots)$. When treating these forces as effective electric fields, within one-step map, the values of all the derivatives of \mathbf{x} are calculated at k-th step. Besides the default algorithms of calculating non-electromagnetic forces, the extendible module of APT provides interfaces of the external forces for users, which can help them design their own pushers for addressing complex physical situations. Most of symplectic methods, on the other hand, are obtained through discrete Hamiltonian or Lagrange systems.

Unlike the Newton equations, the non-electromagnetic forces cannot be separated easily from Hamiltonian or Lagrange equations. Under current version of APT, the external force module cannot be used for such algorithms.

Another important part of the numerical strategy is the calculation of the electromagnetic field. In APT, the electromagnetic fields can be calculated via analytic functions or discrete field data. The analytic field functions include $\mathbf{E}(\mathbf{x}, t)$, $\mathbf{B}(\mathbf{x}, t)$, $\mathbf{A}(\mathbf{x}, t)$, $\phi(\mathbf{x}, t)$, and their derivatives, such as $\partial_i A^j(\mathbf{x}, t)$, $\partial_i \phi(\mathbf{x}, t)$, $\partial_i \partial_j A^k(\mathbf{x}, t)$, $\partial_i \partial_j \phi(\mathbf{x}, t)$, \dots . Self-consistent calculation of APT is implemented through dynamical field models, which evolve under the control of parameters calculated from the phase-space state of all particles. For example, the self-consistent magnetic field of a charged beam is calculated based on line current model. APT first gathers the phase-space information of all particles, and then summarizes the information to obtain the evolution parameters of self-consistent field, such as the position and the strength of the current, and finally updates field models through new parameters. The general model for self-consistent fields can be summarized as $\mathbf{F}[t, \mathbf{x}, c_1(\mathbf{x}_i, \mathbf{p}_i), c_2(\mathbf{x}_i, \mathbf{p}_i), \dots]$, where the index i covers all the simulated particles, and c_1 and c_2 are dynamical parameters. Discrete field data from experiments or simulations can also be used to calculate fields. APT accepts discrete field data distributed on 3-dimensional cubic grids. The local fields of particles are calculated via interpolation functions. To be specific, for discrete vector potential field data A_{ijk}^l , the field at \mathbf{x} is given by $A^l(\mathbf{x}) = \sum_{ijk} A_{ijk}^l W(\mathbf{x} - \mathbf{x}_J)$. Here W is weighting function, i, j, k are indexes on three directions, and l denotes the components of \mathbf{A}_{ijk} .

2.2. The parallelization module

2.2.1. Overview

In order to boost the large-scale application of geometric algorithms, the parallelization module of APT is designed to support parallel computation on different hardware architectures. On supercomputers with Intel architecture, the APT code can be distributed via standard MPI libraries. The GPU version of APT supports the CUDA parallelization method. As a special implementa-

tion, APT-SW supports the many-core acceleration of the Sunway TaihuLight supercomputer. The parallelization module assigns the particle samples to different cores and works in three optional modes, namely, the asynchronous mode, the synchronous mode, and the quasi-synchronous mode. The selection of parallelization modes is determined by specific physical models. The asynchronous parallelization simulates particles independently and is applied to problems with ignorable self-consistent fields of particles. This mode minimizes the communications among processors, and thus possesses highest efficiency among the three methods. For cases with the self-consistent fields, the synchronous parallelization is required. In this mode, particle samples are pushed synchronously and phase-space states of all samples are collected for every step to update self-consistent fields. The quasi-synchronous mode is developed to reduce the resource wastes resulting from communications and is mainly designed for a certain type of physical processes on large-scale computers, where the timescale of self-consistent fields is larger than the timescale of particle motion. For example, during the evolution of runaway beams in tokamaks, the characteristic timescale of Lorentz force is on the order of 10^{-11} s, while the timescale of self-consistent field is on the order of 10^{-1} s. Instead of updating the self-consistent field at every step, the quasi-synchronous model only collects global information and updates the fields at some specified moments, which are determined by the timescale of self-consistent fields and the total physical duration of the simulation. Consequently, the total number of communications is much less than calculation operations. The communication bottleneck can thus be eased when one is dealing with multi-scale self-consistent problems.

2.2.2. APT-SW on the Sunway TaihuLight supercomputer

Recently, the Top 1 supercomputer in the world has been updated as the construction of the Sunway TaihuLight supercomputer in Wuxi, China. Possessing peak performance of 125PFlops, the Sunway TaihuLight becomes the fastest supercomputer in the world [36, 37]. The calculation capability of the Sunway TaihuLight is provided by 40000 SW26010 many-core processors, each

of which has 260 processing elements [37]. Therefore, there are more than 10^7 cores available on this supercomputer. The Sunway TaihuLight supercomputer system has a total storage of 20PB, which makes it possible for the storage and analysis of big data. However, it is not straightforward to distribute a program on this supercomputer, because the architecture of the processor is different from any other CPUs or GPUs. In each SW26010 processor, four master cores and 256 slave cores are integrated. The two types of cores have similar computation ability but different architectures. A program should utilize both the master and slave cores to avoid the waste of the calculation capability of the Sunway TaihuLight. Meanwhile, the communication between a master core and its slave cores becomes the bottleneck of efficiency because of the slow speed of accessing shared memory for slave cores. To improve the memory bandwidth, the SW26010 processor has a 64K local cache memory, also called local data memory (LDM), for slave cores. The slave cores can access the data stored in the LDM with high speed. Consequently, to improve the efficiency, one should appropriately use the LDM to reduce the access of data in shared memory by the slave cores and to minimize the communication between master and slave cores. To achieve these goals, the program should be supported by the master-slave acceleration libraries of the Sunway TaihuLight platform.

As a branch version of the APT code, APT-SW has been successfully distributed on the Sunway TaihuLight supercomputer. APT-SW remains most of the attributes of APT while several modifications have been made to adapt to the computation environment of the Sunway TaihuLight. To implement the master-slave acceleration, the APT-SW source code is divided into two parts, namely, the master-core code and the slave-core code. As is implied by their names, the master-core code is executed by master cores and is in charge of the data I/O, the simulation initialization, the process parallelization, while the slave-core code is run on slave cores, and is responsible for the particle pusher with geometric algorithms, the electromagnetic field module, the external force module, and the extendible module. Through the management functions, the master-core commands can assign computation tasks to slave cores. Specifi-

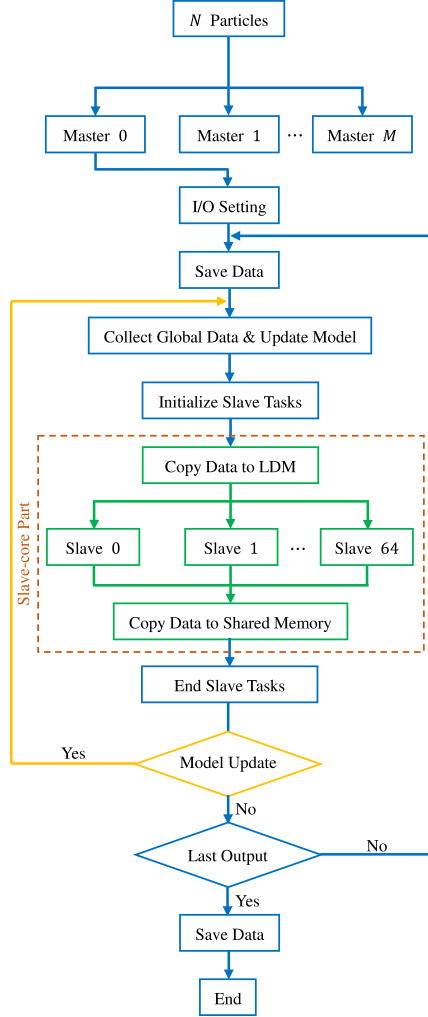


Figure 2: Schematic of master-slave acceleration of APT-SW on the Sunway TaihuLight supercomputer. The total number of particle samples is N , and M is the number of master processes. Because the data can only be written into the file system through master processors and the efficiency of communication between master and slave cores is low, n iterations are divided into m groups based on the users' output configuration, and the data saving executes for m times. In long-term simulations, n is much larger than m . Therefore, the time of master-slave communications can be neglected compared with the iteration time. In the brown dashed box, the slave-core code of APT-SW is depicted. Between two processes of data saving, the master core demands each slave core to execute iterations of n/m times. The quasi-synchronous mode is implemented to overcome the communication bottleneck during simulations of multi-scale self-consistent problems.

cally, the slave-core code is integrated to be one function, and the master-core code determines when and on which slave core the slave-core function should be executed. All the variables used in slave-core code are independent with master-core code to avoid unnecessary access of shared memory by slave cores. The communications between the LDM and shared memory happens only at the stages of initialization, synchronization, data output, and finalization of slave processes.

Figure 2 shows the schematic of master-slave acceleration of APT-SW on the Sunway TaihuLight. The N particle samples are assigned to M master cores, each of which manages 64 slave cores. One slave core executes the iteration of $N/64M$ particle samples. Consequently, the total simulation time is mainly determined by the computation ability and burden of each slave core. Because only the master cores can access the file system, to record the running data, we divide the n iteration steps into m groups, where m is the step number of outputs. When a master core assigns tasks to its slave processes, the data needed are copied to the LDM. Then, the 64 slave cores push their own particles for n/m steps. After that, the data of particles will be gathered back to shared memory for output. As a result, the amount of communications between the master and slave core is proportional to m , and the time resolution of output data is T/m , where T is the physical time in simulations. One can adjust the value of m to find a balance between the time efficiency and the resolution of simulation data. For secular simulations of multi-timescale processes, the total number of iteration n can be very large. It is not necessary to save all the iteration data to analyze the macroscopic behaviors. So the value of m is much smaller than n , which makes the time of master-slave communications ignorable compared with the iteration time. For large-scale simulation on the Sunway TaihuLight computer, the frequency of global data access should be reduced as much as possible in order to avoid the communication delay. As a result, the quasi-synchronous parallel calculation mode is helpful to improve the efficiency of large-scale simulations. By use of APT-SW on the Sunway TaihuLight supercomputer, we have successfully completed the runaway dynamical simulations of 10^{18} particle-steps

which corresponds to 10^{22} floating-point operations. New physical results are obtained, which will be discussed in Sec. 4.

2.3. Use and extend APT

The APT code aims to provide a flexible and extendible software platform for studying and using geometric algorithms. In this section, we introduce APT in two aspects. First, for users who just need to use the built-in functions of the APT code, we show how to install and run the binary file of APT, how to set the parameters via the configuration system, and how to access the output data. Second, for researchers who would like to study their own algorithms or physical models on APT, we provide detailed introductions of the function interfaces, and exhibit the three-step procedure to generate the extended source code of APT via the extendible module.

2.3.1. Installation

The APT code is written in C language, and can be built by compilers supporting the c89 standard. APT depends on the library of Lua-5.2 and Hdf5-1.8. The Lua library has been merged into the source code of APT, while the Hdf5 library, however, should be installed before compiling and running APT. One can visit the official website of the Hdf5 Group to get the source code or pre-built libraries of Hdf5 software [41]. To install APT, users should change the working directory to the root directory of APT source code, and simply run the command:

```
1 make HDF5_ROOT=<Hdf5 Directory>
2 make install PREFIX=<Installation Directory>
```

Here, “HDF5_ROOT” is the root directory of Hdf5 library, and “PREFIX” is the directory of installation. By default, HDF5_ROOT=/usr/local, and PREFIX=./DataAnalysis. In the installation directory, there are the binary file of APT called “APT.out”, the manage configuration file “Config.lua”, the package of main configuration files “pkg/”, the document directory for configuring APT “doc/”, and the auxiliary tool package “tools/”.

2.3.2. The configuration system of APT

The configuration system of APT is built based on the Lua language [42]. Through the Lua library, the global variables in Lua script can be loaded by the main procedure of APT. The interface of APT for Lua scripts supports the transfers of floating-point numbers, integer numbers, strings, and arrays. APT provides a package of main configuration files. Users can select a main configuration file via the “dofile” command in the manage configuration file “Config.lua”. For example, the command

```
1  dofile("./pkg/UniformField.lua");
```

selects the main configuration file called “UniformField.lua” in “pkg/”. Each main configuration file corresponds to one specific task. All the main configuration file templates locate in “pkg/”, and their instructions can be found in the file “doc/MainConfigFiles.txt”. When APT is executed, the manage configuration file is first loaded, which calls the main configuration file selected by a user. Then, the parameters in the main configuration file will be loaded into the parameter container of APT, which control the operation of main procedure.

Figure 3 shows a typical main configuration file of APT, which is used to simulate the motion of charged particles in uniform electromagnetic fields. The parameters are divided into two parts, the physical parameters and the APT dimensionless parameters. As a mandatory rule, all the variables loaded by the main procedure of APT should be dimensionless. The units of main physical quantities are listed in Tab. 1. The physical parameters would not be loaded by APT, and are mainly used to set the physical units. The function, “GAPS_APT_LuaConfig_LoadUnits”, on line 8 in Fig. 3, can help users calculate all the physical units and loads them as Lua global variables listed in Tab. 1. The APT dimensionless parameters presented in Fig. 3 are key variables for obtaining correct simulation results. Actually, the dimensionless parameters in one main configuration file form a subset of the parameter container of APT. They might be used anywhere in the main procedure. While writing a main configuration file, users just need to ensure that all the dimensionless param-

Names	Symbols	Units	Lua Global Variable
Mass	m	m_e	Unit_Mass
Charge	q	e	Unit_Charge
Time, Proper Time	t, τ	m_e/eB_0	Unit_Time
Position, Canonical Coordinate	\mathbf{x}, \mathbf{X}	$m_e c/eB_0$	Unit_Space
Mechanical, Canonical Momentum	\mathbf{p}, \mathbf{P}	$m_e c$	Unit_P
Velocity	\mathbf{v}	c	Unit_V
Electric field	\mathbf{E}	$B_0 c$	Unit_E
Magnetic field	\mathbf{B}	B_0	Unit_B
Vecter field	\mathbf{A}	$m_e c/e$	Unit_A
Scalar field	ϕ	$m_e c^2/e$	Unit_Phi
Hamiltonian, Energy	\mathcal{H}, \mathcal{E}	$m_e c^2$	Unit_Energy

Table 1: Units of all the physical quantities used in this paper. m_e is the rest mass of a particle, e is the elementary charge, c is the speed of light, and B_0 is the reference strength of magnetic field. The variables in last column can be accessed in Lua script after the function “GAPS_APT_LuaConfig_LoadUnits(B_0)” is called.

ters are defined and assigned with correct value. Then, they can organize the expressions in main Lua configuration files in any ways they like. Because of the flexibility of Lua script, the configuration system of APT provides user with large freedom during parameter setting. The main procedure of APT also automatically generates two scripts, “LoadCalInfo.m” and “LoadCalInfo.py”, for matlab and python, through which users can load all the inputted parameters during data analysis.

In Fig. 3, all parameters are provided with introductions. Most of them are easy to understand. Parameters named with prefixes “EMField”, “ExtForce”, “Pusher”, and “Init” are related to the configurations of the electromagnetic module, the external force module, the particle pusher module, and the initialization module, respectively. “EMField_Type” sets the type of electromagnetic fields. The available electromagnetic fields and their necessary setting parameters are listed in the file “doc/EMFields.txt”. The parameters for enabling the calculations of external non-electromagnetic forces are not listed in Fig. 3. These variables are named as “ExtForce_Cal_<Name>”. For example, to open the calculation of radiation force of particles, one needs to set “ExtForce_Cal_RadLarmor” as 1. The file “doc/ExternForces.txt” contains information for available forces. “Pusher_Type” sets the type of pushers. The introductions for all available pushers can be found in the file “doc/Pushers.txt”. The methods for initializing the position and momentum of particles are determined by “Init_X_Type” and “Init_P_Type”, respectively. For details of available initial conditions and their parameters, one can refer to the files in directory “doc/Initialization/”. The other parameters also play key roles in the operation of APT. For example, APT saves data every “SaveSamplePeriod” steps, and “Open_Work_Cal” can enable the calculation of works of electric field and other non-electromagnetic forces if it is set to be 1. Another important parameter we need to introduce is “RunCheckPoint”. If its value is 1, APT can execute data recovery from the point of interruption and re-initialization automatically. This function is necessary for large-scale simulations on supercomputers because the probability of system exceptions increases with the scale

of parallelization. For the introductions of all parameters in APT, users can refer to the file “doc/Parameters.txt”.

In current version, APT has integrated various volume-preserving and symplectic algorithms for both classical and relativistic systems. The volume-preserving algorithms (VPA) include both non-relativistic and relativistic VPAs of different orders [13, 15, 19, 20]. The symplectic algorithms built in APT contain the canonical symplectic Euler algorithm, the implicit mid-point symplectic algorithm, the K-symplectic algorithm, and the explicit symplectic algorithms based on generating functions [23, 31, 32, 43]. Canonical or non-canonical symplectic structures are preserved during iteration by these symplectic algorithms. Through the preservation of geometric structures, the geometric algorithms in the particle pusher module equip APT with long-term stability. For example, it has been verified that VPAs can trace the dynamics of particle correctly for tens of billion steps [15, 19, 20, 38, 39]. Besides the geometric algorithms, traditional algorithms, such as the Runge-Kutta algorithms of different orders, are also available in APT. These traditional algorithms can be used as references for the analysis of new algorithms.

In the electromagnetic field module, several configurations have been integrated, including the tokamak field, the terrestrial magnetic field, the uniform field, the radially non-uniform magnetic field, and the electric oscillator field, etc. Besides the electromagnetic field function, the scalar and vector potentials are also available in order to support the usages of some geometric algorithms. In current version of APT, self-consistent field calculations for runaway electrons and charged beams have been implemented. If setting “EMField_Type” as -1, users can use discrete field data obtained from experiments or simulations to push particles. APT can accept Hdf5 data files containing discrete electromagnetic field data $EB = (\mathbf{E}, \mathbf{B})$ or potential data $A^\alpha = (\phi, \mathbf{A})$ on 3D cubic grids. The structure and necessary datasets of the Hdf5 file are listed in Tab.2. EB is used by algorithms derived from Newton equations, while A^α is needed by symplectic algorithms. To simplify the generation of discrete field data file, in “tools/”, we have implemented a mat-

```

1  -- Configuration File: Charged particles in uniform electromagnetic fields
2
3  -- Physical Parameters
4  B0 = 1; -- Magnetic strength (T)
5  E0 = 1; -- Electric strength (V/m)
6  R0 = 1.7; -- Major radius of torus (m)
7  a  = 0.4; -- Minor radius of torus (m)
8  GAPS_APT_LuaConfig_LoadUnits(B0); -- Load all units based on B0
9
10 -- APT Dimensionless Parameters
11 num_steps = 1000; -- Simulate 1000 steps
12 num_total_particles = 1; -- Simulate 1 particle
13 OpenDataSaving = 1; -- Open data saving
14 SaveSamplePeriod = 1; -- Sample period for saving data
15 Pusher_Type = 0; -- Select pusher 0 (Volume-preserving Algorithm)
16 EMField_Type = 0; -- Select electromagnetic field 0 (Uniform Field)
17 EMFeild_Uniform_AngleEB = 0; -- Angle between B and E is 0
18 EMField_B0 = B0/Unit_B; -- Set dimensionless magnetic strength
19 EMField_E0 = E0/Unit_E; -- Set dimensionless electric strength
20 EMField_Cal_B = 1; -- Open calculation of magnetic field
21 EMField_Cal_E = 1; -- Open calculation of electric field
22 Init_X_Type = "Constant"; -- Initial position distribution is "Constant"
23 Init_X_Constant_X0 = {0, 0, 0}; -- Set boundary
24 Init_P_Type = "Constant"; -- Initial momentum distribution is "Constant"
25 Init_P_Constant_P0 = {1, 0, 0.1}; -- Value of constant momentum
26 dT = 0.1; -- Step time length
27 RunCheckPoint=0; --Continue calculation from break point

```

Figure 3: An example of configuration files (pkg/UniformField.lua). This file provides all the parameters for simulating charged particles moving in a uniform electromagnetic field.

Dataset	Dimension	Description
/Order	1×1	Types of fields: -1 for EB , 1 for A^α
/N_grid	4×1	Numbers of spacetime grids: (n_x, n_y, n_z, n_t)
/DX	1×1	Dimensionless length of space grid
/DT	1×1	Dimensionless time step length
/OriginPoint	3×1	Origin point coordinate of field region
/Data	$n_t \times M$	Discrete data of fields

Table 2: Data structure of Hdf5 file for inputting discrete field data. EB is a 6-dimension array containing values of electromagnetic fields, namely (\mathbf{E}, \mathbf{B}) , and A^α is a 4-dimensional array containing scalar and vector potentials, namely (ϕ, \mathbf{A}) . n_x, n_y and n_z denote numbers of spatial grids on each direction, and n_t is the number of time steps of discrete field data. For static fields, one should set $n_t = 1$. x_0, y_0 , and z_0 are dimensionless coordinates of the origin point of field region. For each moment, the data of a tensor F_{ijk}^l should be rewritten as a 1D array F_J based on the index mapping $J = l + D[i + n_x(j + n_y k)]$, where D is the number of components of \mathbf{F} , i, j, k are indexes of grids on three directions, and l is the index of components of \mathbf{F} . $M = D \times n_x \times n_y \times n_z$ is the number of data for each moment. The value of D can be set as 6 or 4 for EB or A^α , respectively.

lab function “GAPS_APT_CreateDiscreteDataFile.m”, which can transfer a $D \times n_x \times n_y \times n_z \times n_t$ 5-dimensional matlab array into an APT-readable Hdf5 file. The full path of inputted Hdf5 file can be passed to APT via parameter “EMField_Discrete_Filename”.

The external force-field module loads non-electromagnetic forces into the dynamical simulation of particles. Various external forces including synchrotron radiation force, collisional force, bremsstrahlung force, and gravitation field have been built in the APT code. To calculate the random collisional force, the Langevin Coulomb collision model is adopted, which is an energy-preserving random numerical method for plasmas without electric field [35].

Through the parameters “Init_X_Type” and “Init_P_Type”, one can set different types of initial distributions. The initialization module provides several commonly used methods of statistical sampling. For position sampling, APT supports uniform distributions of different shapes, including cuboid, cylin-

der, and torus. For momentum sampling, APT supports two-stream sampling, normal-distribution sampling, etc. The initialization module facilitates the usage of APT in complex realistic physical problems.

2.3.3. The architecture of Hdf5 output data

The Hdf5 library provides a file-system-like way of reading and writing data [41], i.e., one can access the data like manipulating a file in Linux operation system. This mechanism can simplify the procedure of accessing and analyzing data. The Hdf5 format is supported by most of the popular data-analysis tools, such as Matlab and Python.

APT stores simulation data in an Hdf5 file called “Data.h5”. The basic dataset is “/PTC”, which contains all the information of particles. “/PTC” is a $L_s N_{ptc} \times N_{steps}$ 2-dimensional matrix. Here N_{ptc} and N_{steps} are respectively the number of particles and the number of saved steps. $L_s = 11$ is the number of data for one particle. The sequence of data for one particle is $S_{die}, t, x, y, z, p_x, p_y, p_z, a_x, a_y, a_z$. If the value of S_{die} is 1, the particle is “dead” and the program stops updating its data. The main procedure of APT changes the value of S_{die} to 1 if a particle is out of boundary of discrete fields. The other data are time (t), Cartesian coordinates (x, y, z), momentum/velocity (p_x, p_y, p_z), and acceleration (a_x, a_y, a_z). All of them are dimensionless.

If enabling the calculations of electromagnetic fields or other external fields, users can also find datasets in “Data.h5” named after these forces in the Hdf5 file. They are all $3 \times N_{steps}$ matrices. Moreover, if the work calculation is enabled, the data of works for all forces, except magnetic force, will be stored in datasets named as “/Work_<Name>”, where, <Name> is the name of forces. These work datasets are “ $1 \times N_{steps}$ ” matrices.

2.3.4. The interfaces of APT

Once being familiar with the installation procedures, the configuration system, and the data format, users can benefit from all the built-in resources of algorithms and physical modules of APT. However, they can do more than that.

In the field of scientific calculation, researchers usually need to extend codes to achieve their personal goals. Sometimes, they need to understand the architecture of a code and modify different places of the source code. This process takes researchers a lot of time and reduces the efficiency for researching. And, because there is no standard rule for modification and extension, most of the modified codes cannot be used easily by other researchers. APT aims to improve the efficiency of extending the source code, integrate novel works from different fields, and finally provide researchers a platform of cooperation on which the geometric algorithms can be studied and used more conveniently. To achieve this goal, the APT project designs standard function interfaces and naming rules for the containers of variables, pushers, electromagnetic fields, external forces, and initialization methods. Before showing how to extend APT, we first give a detailed description about the interfaces of APT in this part.

The parameter container. As we have introduced before, the operation of APT is governed by lots of control parameters loaded from configuration files. Therefore, the parameter container is a vital part of APT, which appears in most of interfaces. The parameter container is a structure named “Gaps_IO_InputsContainer”, whose fields compose the complete set of input parameters. Its definition is:

```

1  typedef struct{
2      long num_steps;
3      double EMField_B0;
4      char Init_X_Type[50];
5      double Init_P_Constant_P0[3];
6      // ...
7  }Gaps_IO_InputsContainer;
```

Through this structure, developers can access all the control parameters.

The particle structure. Like the parameter container structure, the particle structure is also an important data type for interfaces of APT, which is named as “Gaps_APT_Particle”. The particle structure contains all the data of a

particle, such as time, position, momentum, acceleration, and electromagnetic field. Through the particle structure, developers can access all the particle data and functions of electromagnetic fields and external forces. APT provides a set of functions for obtaining data in a particle structure. These functions take the pointer of a particle structure as its input, and return the pointers of corresponding data. They are named following the format “GAPS_APT_Get<Name><Dim>”, where <Name> is the abbreviation of a physical quantity, and <Dim> is a integer denoting the dimension of data. Here is a typical example for obtaining the pointer of 4-dimensional space time:

```
1 double * GAPS_APT_GetX4(Gaps_APT_Particle *pPtc);    // SpaceTime
```

The complete list of these functions is given in Tab. 3.

The electromagnetic field interface. Geometric algorithms usually have complex forms. Sometimes high-order derivatives and integral calculation of field functions are needed. The electromagnetic field module aims to provide a unified interface for calculating not only electromagnetic field functions, but also their integrals and derivatives. Therefore, the prototype of field functions is defined as:

```
1 typedef int (*Gaps_APT_Field)(double *pTensor, double *pSpaceTime4, int Order,
2                               Gaps_IO_InputsContainer *pInputs);
```

The function interface uses the 4-dimensional representation, which takes 4-dimensional spacetime, $X^\alpha = (t, \mathbf{X})$, as input parameters and returns tensors of different orders. Other necessary inputs are the pointer of parameter container and the order of the tensor. The definitions of tensors in APT are different from ordinary conventions, which are listed in Tab. 4. Tensors of 3-order can be calculated by most of electromagnetic field functions to support the use of some high order symplectic algorithms. The template for electromagnetic field functions is

```
1 #include "APT_AllHeaders.h"
2 int GAPS_APT_Field_<Name>(double *pTensor, double *pSpaceTime4, int Order,
```


Name	Physical quantity
GAPS_APT_GetDie1	Marker of life
GAPS_APT_GetCharge1	Charge
GAPS_APT_GetMass1	Mass
GAPS_APT_GetS1	Proper time
GAPS_APT_GetX4	Space time
GAPS_APT_GetP4	4-momentum
GAPS_APT_GetCanP4	4-canonical-momentum
GAPS_APT_GetA4	4-vector-potential
GAPS_APT_GetT1	Time
GAPS_APT_GetX3	Position
GAPS_APT_GetP3	Momentum
GAPS_APT_GetCanP3	Canonical momentum
GAPS_APT_GetA3	Vector potential
GAPS_APT_GetGamma1	Lorentz factor
GAPS_APT_GetE3	Electric field
GAPS_APT_GetB3	Magnetic field
GAPS_APT_GetAclr3	Acceleration
GAPS_APT_GetEwork1	Work of electric field
GAPS_APT_GetFieldFunc	Function pointer of EM field

Table 3: List of functions for accessing data from the particle structure.

Tensor	Order	Dimension	Length of data array
EB	-1	6	6
A^α	1	4	4
$\partial_\beta A^\alpha$	2	4	16
$\partial_\beta \partial_\gamma A^\alpha$	3	4	64
\dots	\dots	\dots	\dots

Table 4: Definitions of tensors in APT. $A^\alpha = (\phi, \mathbf{A})$ is the 4-potential vector, and ∂_α denotes the derivative operation with respect to the α -th component of spacetime. Definitions of tensors corresponding to A^α are the same with ordinary conventions. The electromagnetic tensor $F_{\alpha\beta} = \partial_\alpha A_\beta - \partial_\beta A_\alpha$ is transformed to a 6-dimensional 1-order array $EB = (\mathbf{E}, \mathbf{B})$ in APT to avoid the confusion of the “4-dimensional 2-order” tensor.

```

3           Gaps_IO_InputsContainer *pInputs)
4   {
5       /**Step 1: Set the maximum tensor order**/
6       int MaxOrder = 1;
7       /**Step 2: Declare and calculate intermediate variables**/
8       /**Step 3: Calculate EB: Order=-1**/
9       if(-1 == Order)
10      {
11          if(pInputs->EMField_Cal_E)
12          {
13              //Calculate E and assign values to pTensor[0]-pTensor[2]
14          }
15          if(pInputs->EMField_Cal_B)
16          {
17              //Calculate B and assign values to pTensor[3]-pTensor[5]
18          }
19      }
20      /**Step 4: Calculate 4-vector-potential: Order=1**/
21      if(1 == Order)
22      {
23          //Calculate A and assign values to pTensor[0]-pTensor[3]
24      }
25      /**Step 5: Error detection**/

```

```

26     if(MaxOrder < Order || 0 == Order)
27     {
28         fprintf(stderr, "ERROR: In function GAPS_APT_Field_<Name>.
29             This field function does NOT support tensor of
30             0-order or order larger than %d.\n", MaxOrder);
31     }
32     return 0;
33 }

```

The formal parameter “pTensor” in field function interface points to the head of a 1-dimensional array, which contains the data of tensors. The length of “pTensor” is determined by both the dimension and the order of a tensor. For a n -order m -dimensional tensor, the length of “pTensor” is $L_{fld} = m^n$, see Tab. 4. APT has implemented functions that can return the components of “pTensor” through its index array, namely,

```

1  double GAPS_APT_TensorValue(double *pTensor, int *pIndex, int Dim, int Order);
2  double *GAPS_APT_TensorPointer(double *pTensor, int *pIndex, int Dim, int Order);

```

“pIndex” is an integer array with n elements, which contains the indexes of tensor. The “Dim” and “Order” are the dimension and the order of a tensor, respectively.

Some geometric algorithms need to calculate the definite integral of field functions [23]. APT provides a numerical quadrature function to accomplish the definite integral of arbitrary components of arbitrary field tensor functions, namely,

```

1  double GAPS_APT_FieldIntegral(int n, Gaps_APT_Particle *pPtc,
2                                int Order, int *pIndex, int idxInt,
3                                double *pST0, double *pST1,
4                                Gaps_IO_InputsContainer *pInputs);

```

Here, “n” defines the number of intervals within the integral domain, “Order” is the order of tensors, “pIndex” is an array denoting the component the integrand tensor, “idxInt” sets which component of spacetime is the integral variable, and “pST0” and “pST1” are the start and end points of integral domain. For

example, to calculate the integral $\int_{t_0}^{t_1} EB_1 dt = \int_{t_0}^{t_1} E_y dt$ for $\mathbf{X} = (x_0, y_0, z_0)$, the corresponding codes when implementing a new pusher are

```

1  int Order=-1;//Order of EB is -1
2  int pIndex[1]={1};//Integrand is Ey
3  int idxInt=0;//The 0th component of spacetime is t.
4  int n=512;
5  double pST0[4]={a,x0,y0,z0};
6  double pST1[4]={b,x0,y0,z0};
7  double result;
8  result=GAPS_APT_IntegralField(n,pPtc,Order,pIndex,idxInt,pST0,pST1,pInputs);

```

Here, “pPtc” points to a particle structure, “pInputs” points to the parameter container.

APT approximates the self-consistent field of particles through mapping the phase-space states of all particles to several dynamical parameters of field functions. Generally, for any self-consistent model, one needs the information of all particles at a moment. Therefore, we provide a function to gather the information of all particles, namely,

```

1  int GAPS_APT_GatherPtcInfo(double *pData);

```

This function returns the positions and momenta of all particles into a $6N$ -dimensional array “pData”. The data sequence in “pData” is $\mathbf{x}_0, \mathbf{p}_0, \mathbf{x}_1, \mathbf{p}_1, \dots, \mathbf{x}_{i-1}, \mathbf{p}_{i-1}$. Through this function, user can accomplish different approximate self-consistent models of particle dynamics. This simplified self-consistent model of APT is designed to find a compromise between efficiency and accuracy when the self-consistent calculation cannot be avoided. For many specific physical processes, this method can still provide useful physical information with high efficiency.

Finally, for discrete field data, the field function interface is the same with analytical functions. The local fields of a particle are calculated through the interpolation of discrete data. Users need not to know the details of discrete field structure, but can use the field function of discrete field data just like the

analytical field functions.

The external non-electromagnetic force interface. The prototype of non-electromagnetic force functions is:

```
1  typedef int (*Gaps_APT_ExtForce)(double *pForce3, Gaps_APT_Particle *pPtc,
2                                     Gaps_IO_InputsContainer *pInputs);
```

The external force module works with the algorithms derived from Newton equations. The dimension of force vector is limited to be 3. The pointer of particle structure is passed into the force functions to provide all needed data. The constant coefficients of a force can be given through the parameter container. The template of external non-electromagnetic force functions is

```
1  #include "APT_AllHeaders.h"
2  int GAPS_APT_ExtForce_<Name>(double *pForce3, Gaps_APT_Particle *pPtc,
3                                Gaps_IO_InputsContainer *pInputs)
4  {
5      /**Step 1: Get pointers of particle data**/
6      double *pX = GAPS_APT_GetX3(pPtc);
7      /**Step 2: Get constant coefficients from pInputs**/
8      /**Step 3: Calculate and assign values to pForce3[0]~pForce3[2]**/
9      return 0;
10 }
```

In APT, each external force is assigned with a serial integer number. Developers can calculate the value of a force through function

```
1  int GAPS_APT_CalExtForce(double *pForce3, int Type, Gaps_APT_Particle *pPtc,
2                             Gaps_IO_InputsContainer *pInputs);
```

This function return the value of the force with serial number “Type”. To update all the force data in particle structure, the function

```
1  int GAPS_APT_UpdatePtcData_ExtForce(Gaps_APT_Particle *pPtc,
2                                       Gaps_IO_InputsContainer *pInputs);
```

is useful. If users want to obtain the sum of all the loaded forces and update the force data at the same time, they can call

```

1  int GAPS_APT_MergeExtForce(double *F_ext3, Gaps_APT_Particle *pPtc,
2                                Gaps_IO_InputsContainer *pInputs);

```

These three functions are useful during implementing a new particle pusher.

The particle pusher interface. The particle pusher interface is the most important part of APT. The prototype of particle pusher functions is defined as

```

1  typedef int (*Gaps_APT_ParticlePusher)(Gaps_APT_Particle *pPtc,
2                                          Gaps_IO_InputsContainer *pInputs);

```

When writing a pusher function, one should ensure the pusher can finish two tasks: 1) for all pushers, update the time, position, and the mechanical momentum of a particle through an algorithm, 2) for pushers derived from Newton equations, update electromagnetic data and non-electromagnetic force data. Here is a template for a particle pusher

```

1  #include "APT_AllHeaders.h"
2  int GAPS_APT_Pusher_<Name>(Gaps_APT_Particle *pPtc,
3                              Gaps_IO_InputsContainer *pInputs)
4  {
5      /**Step 1: Get pointers of particle data**/
6      double *pT = GAPS_APT_GetT1(pPtc); //Time
7      double *pX = GAPS_APT_GetX3(pPtc); //Position
8      double *pP = GAPS_APT_GetP3(pPtc); //Momentum
9      double *E = GAPS_APT_GetE3(pPtc); //Electric field
10     double *B = GAPS_APT_GetB3(pPtc); //Magnetic field
11     Gaps_APT_Field FieldFunc= GAPS_APT_GetFieldFunc(pPtc);
12     /**Step 2: Get parameters from pInputs**/
13     double dT=pInputs->dT; //Time step length
14     /**Step 3: Update pT, pX, pP through an algorithm**/
15     /**Step 4: Update electromagnetic field data**/
16     GAPS_APT_UpdatePtcData_EB(pPtc,pInputs);
17     /**Step 5: Update force data**/
18     GAPS_APT_UpdatePtcData_ExtForce(pPtc,pInputs);
19     return 0;
20 }

```

While implementing a new pusher function, one needs not to know the specific forms of electromagnetic fields or external forces, which have been built in other modules. They just need to focus on their own job of algorithms.

The initialization interface. Researcher can add different approaches of initialization into APT through initialization interface. The interfaces for position and momentum initialization are

```

1  int GAPS_APT_SetParticlePosition_<Name>(Gaps_APT_Particle *pPtc,
2                                          Gaps_IO_InputsContainer *pInputs);
3  int GAPS_APT_SetParticleMomentum_<Name>(Gaps_APT_Particle *pPtc,
4                                          Gaps_IO_InputsContainer *pInputs);

```

“<Name>” denotes the name of initialization methods. For example, the function for Maxwell distribution of momentum is “GAPS_APT_SetParticleMomentum_Maxwell”, which can be loaded by APT if the parameter “Init_P_Type” in configuration file is set as “Maxwell”. The control parameters of generating distributions can be accessed via “pInputs”. The template of initialization function is

```

1  #include "APT_AllHeaders.h"
2  int GAPS_APT_SetParticlePosition_<Type>(Gaps_APT_Particle *pPtc,
3                                          Gaps_IO_InputsContainer *pInputs)
4  {
5      /**Step 1: Get pointers of coordinates**/
6      double *pX = GAPS_APT_GetX3(pPtc);
7      /**Step 2: Get parameters from pInputs**/
8      /**Step 3: Generate random number and assign them to pX*/
9      return 0;
10 }

```

2.3.5. Extend APT

In this part, we give a detailed introduction on how to extend the configuration parameters, the electromagnetic functions, the external forces, the particle pushers, and the initialization approaches of APT.

A brief description of the extendible module. The extendible module of APT is implemented based on Bash-script. Following three steps, users can conveniently build a new version of APT for new applications, see Fig. 1. First, write new C functions for electromagnetic fields, external forces, algorithms, or initialization approaches in specified directories of APT. Second, modify the file “script/ADD” and tell APT the names, types and introductions of these new functions, and the necessary parameters. Third, run the script named “Generation.sh”. Then, all the source codes and documents will be generated automatically. The extended version of APT can be compiled directly. After writing a Lua configuration file, users can test and use their own functions immediately. The detailed three-step procedures are listed as follows.

Step 1: Write new function files. When introducing the interfaces of APT, we have provided templates for electromagnetic field functions, external force functions, particle pusher functions, and initialization functions. Users need to organize one function in a single file. Then they should move new function files into corresponding directories. The electromagnetic function files locate at “src/EMField/”, the external force function files locate at “src/ExtForce”, the particle pusher function files are placed at “src/Pusher”, and the initialization function files are in “src/Initialization”.

Step 2: Add function descriptions and new parameters. Now developers should add descriptions for new functions via the management script of the extendible module, “script/ADD”. There are several commands provided by APT to conveniently accomplish this job, namely,

1	Add_EMField	"<Name>"	"<Parameters>"	"<Notes>"	"<Info>"
2	Add_ExtForce	"<Name>"	"<Parameters>"	"<Notes>"	"<Info>"
3	Add_Pusher	"<Name>"	"<Parameters>"	"<Notes>"	"<Info>"
4	Add_InitMethod	"<Class>"	"<Name>"	"<Parameters>"	"<Notes>" "<Info>"

For example, to add an electromagnetic function called “GAPS_APT_Field_Uniform”, the full command is


```
1 Add_EMField "Uniform" "EMFeild_Uniform_AngleEB" "MaxOrder:3" "Uniform EM field"
```

Developers should notice that <Name> here dose not denote the full name of functions but the name without prefix. <Parameters> is a list of all necessary parameters used in new functions, and <Info> is a short introduction about the function. <Notes> should contain important information to help users use the function correctly. The first input <Class> of “Add_InitMethod” can be “X” or “P”, which denote the initialization functions for positions or momenta, respectively.

For new functions, additional parameters might be used. For example, the parameter for setting the temperature of Maxwell distribution is “Init_P_Maxwell_Temp”. APT requires that all the extended parameters are named following the standard of APT. Parameters for electromagnetic field, external non-electromagnetic forces, particle pushers, and initialization approaches should be named as “EMField_<Name>_<Parameter>”, “ExtForce_<Name>_<Parameter>”, “Pusher_<Name>_<Parameter>”, and “Init_<X/P>_<Name>_<Parameter>”, respectively, where <Name> denotes the name of functions, and <Parameter> can be designed freely by users. The command for adding new parameters in the file “script/ADD” is

```
1 Add_Inputs "<Type>" "<Dim>" "<Name>" "<Introduction>"
```

<Type> is the type of parameters, which can be “double”, “long”, “char”. <Dim> is a integer larger than 0 and denotes the dimension of parameters. <Name> is the name of parameters. <Introduction> is a short description of a parameter, which can help users understand the functions of parameters. If <Dim> is 1, the extendible module will declare the parameter as a single variable; if <Dim> is larger than 1, the parameter is declared as an array.

Step 3: Update source code via one command. After modifying the file “script/ADD”, there is only one last step needed to update the source code, namely, changing directory to “script/” and run the command

```
1 ./Generate.sh
```

Then all the new functions will be integrated into APT, and the documents in “doc/” will also be updated at the same time. The new version of APT source code can be directly compiled. User can also optionally provide new main configuration files in “pkg/”. The introductions of them should be written in “doc/MainConfigFiles.txt”.

By use of the extendible module, researchers from different fields can conveniently focus on their own tasks and use the components provided by others directly. For example, researchers from the plasma physics, accelerator physics, space science, and fusion energy can add the customized electromagnetic configurations and directly use the advanced geometric algorithms provided by computational mathematicians. The complex physical field configurations can be used by mathematicians to analyze their newly developed algorithms. This extendible module can thus boost the integration of new results from different fields.

3. Applications of APT in Scientific research

The APT code has been used in the studies of new algorithms and the simulations of a variety of important plasma processes. Due to the secular stability provided by the geometric algorithm kernel, APT can solve many multi-scale and nonlinear problems that cannot be addressed by traditional simulation methods, which stimulates the discoveries of new physical phenomena. In this section, we exhibit the prospects of APT in two applications, namely, the secular dynamics of runaway electron in tokamak and the distribution evolution of energetic particles in Van Allen belts.

3.1. *The Secular Dynamics of Runaway Electrons*

Runaway electrons are energetic charged particles generated in tokamaks which are the most prospective devices for controlled fusion energy [44, 45]. During the operation of tokamaks, fast shutdown, disruptions, and strong current drive can induce the generation of large amounts of runaway electrons

[46–60]. Due to the acceleration of the induced loop electric field, runaway electrons carrying energies of tens of MeVs have been reported in various experiments [61–64]. The existence of runaway electrons is a potential threat to safety operation of tokamak devices. To study the runaway process, the relativistic effect and the synchrotron radiation cannot be neglected. The runaways reach the synchrotron energy limit when the acceleration of the electric field is balanced out by the synchrotron radiation dissipation [14, 65–67]. Both the detailed dynamical behaviors and the rules of energy limit of runaway electrons are important topics in the field of fusion energy.

The runaway dynamics is a typical multi-scale process, which involves timescales from characteristic time of Lorentz force (10^{-11} s) to energy balance time (1 s) [39, 67]. The runaway dynamics thus spans about 11 orders of magnitude in timescale. To eliminate the trouble of multi-timescale, traditional methods average out the motion in small timescale, which simplifies the problem but loses physical information. However, with the secular stability of geometric algorithms, APT can simulate directly the full-orbit dynamics which needs more than 10^{12} time steps. Correspondingly, runaway dynamical pictures containing information of all timescales have been produced. Especially, the discovery of neoclassical collisionless pitch-angle scattering brings a novel understanding about runaway behaviors and results in new laws of energy limit.

Figure 4 depicts the snapshots of runaway orbit projected on poloidal plane at different moments simulated by APT. Besides the Guan-Slide effect, this full-orbit result also exhibits clearly the detailed ripple structures in small timescale [14, 39]. To obtain Fig. 4, we use the relativistic volume-preserving algorithm in APT. Because the runaway dynamics involves the synchrotron radiation, the external force-field module of APT is also used. The tokamak field configuration file of APT provides the needed field given by

$$\mathbf{B} = -\frac{B_0 R_0}{R} \mathbf{e}_\xi - \frac{B_0 \sqrt{(R - R_0)^2 + z^2}}{qR} \mathbf{e}_\theta, \quad (14)$$

$$\mathbf{E} = E_l \frac{R_0}{R} \mathbf{e}_\xi, \quad (15)$$

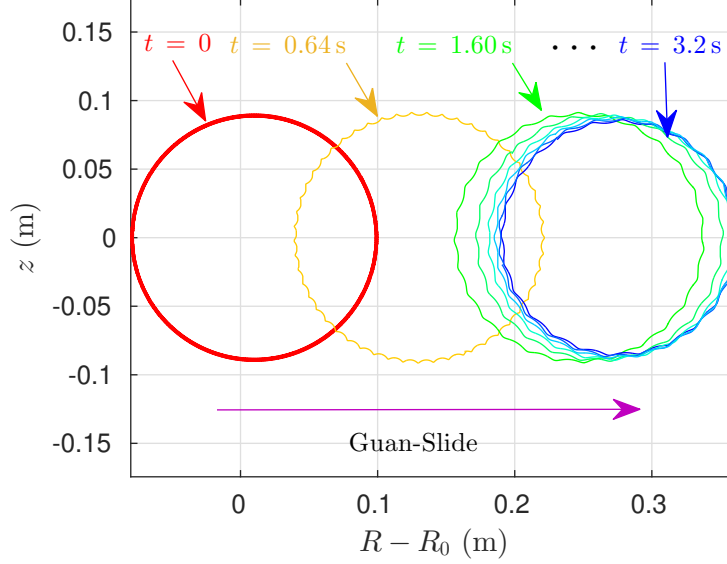


Figure 4: Full-orbit snapshots of runaway orbit projected in the poloidal plane at different moments. The configuration of field is determined by $R_0 = 1.7$ m, $a = 0.4$ m, $q = 2$, $B_0 = 2$ T, and $E_l = 0.2$ V/m. The runaway electron is initially sampled with momentum $p_{\parallel 0} = 5 m_0 c$, $p_{\perp 0} = 1 m_0 c$ at $R = 1.8$ m, $\xi = z = 0$. Besides the neoclassical radial drift, the ripple structures are obviously exhibited.

where, \mathbf{e}_ξ and \mathbf{e}_θ are respectively the toroidal and poloidal unit vectors, R_0 is the major radius, q denotes safety factor, E_l is the strength of loop electric field, and B_0 is the magnitude of background magnetic field. In calculation, we set parameters based on a typical tokamak, that is $R_0 = 1.7$ m, $a = 0.4$ m, $q = 2$, $B_0 = 2$ T, and $E_l = 0.2$ V/m. The initial position of a runaway electron is chosen as $R = 1.8$ m, $\xi = z = 0$, and the initial parallel and perpendicular momenta are set as $p_{\parallel 0} = 5 m_0 c$ and $p_{\perp 0} = 1 m_0 c$ respectively. The time step of simulation is set as $\Delta t = 1.9 \times 10^{-12}$ s. The total number of iteration steps is thus about 1.6×10^{12} . The long-term stability of APT ensures the correctness of simulation results even after 10^{12} steps.

3.2. Energetic Particles in Van Allen Radiation Belt

Since its discovery in 1958, the Van Allen radiation belts have been an important topic of geophysics [68]. The Van Allen belt is a region about several R_E s away from the surface of earth, where R_E is the radius of earth at the equator. Large amounts of particles carrying energies of several MeVs are confined in the radiation belt. These energetic particles do harm to the spacecraft as well as the satellites. The mechanism of acceleration of energetic particles in radiation belts is still not clear, even though many works have been done on this problem [69, 70].

APT has offered an outstanding platform for studying the statistical behaviors and the acceleration mechanisms of radiation-belt particles. The background terrestrial field is approximated by

$$\mathbf{B}(\mathbf{x}) = \frac{B_0 R_0^3 z}{(R^2 + z^2)^2} \mathbf{e}_R + \frac{B_0 R_0^3}{R^2 + z^2} \left(-\frac{R}{R^2 + z^2} + \frac{1}{2R} \right) \mathbf{e}_z.$$

The corresponding vector field is

$$\mathbf{A}(\mathbf{x}) = \frac{B_0 R_0^3}{2(R^2 + z^2)} \mathbf{e}_\theta, \quad (16)$$

where $R_0 = 6.6R_E$ and $B_0 = 2B_{surf}/6.6^3$, $R_E = 6370000$ m is the radius of earth, and $B_{surf} = 3.12 \times 10^{-5}$ T is the magnetic field on surface of earth. The parallelization module is used to achieve large-scale statistical simulations on supercomputers. Users can choose different geometric algorithms, adopt various initial statistical samplings, and test different electromagnetic-wave acceleration processes in APT.

We choose the symplectic Euler algorithm for relativistic charged particles to simulate the collective evolution of energetic electrons in the background magnetic field of earth. Initially, 10^4 particles are uniformly sampled in the region $3.3R_E \leq R \leq 3.7R_E$ and $-0.2R_E \leq z \leq 0.2R_E$. The initial Lorentz factors of particles are given by a normal distribution with the average value $\mu = 0.6$ MeV and the standard deviation $\sigma = 0.5$ KeV, and the initial momenta are sampled uniformly within $-1 \leq p_{\parallel}/p \leq 1$. The time step is about 5.24×10^{-6} s, and the number of steps is 2.8×10^5 . The diffusion process of energetic electrons

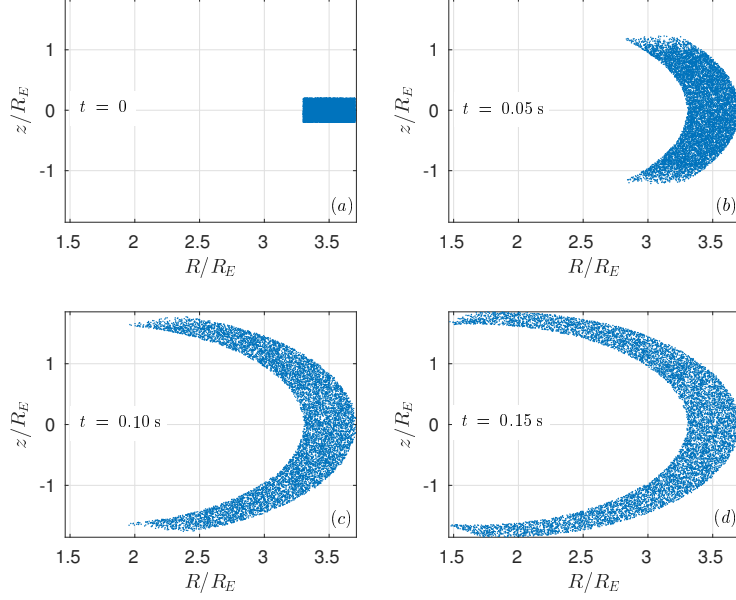


Figure 5: The diffusion process of energetic electrons in Van Allen belts.

in Van Allen belt of earth is shown in Fig. 5. Since the confined particles in the initial region have different momenta and phases, they do not move together but spread in the earth magnetic field. The profile of distribution at $t = 0.15$ s shows the shape of radiation belts, which reveals the formation of Van Allen belt.

4. Large-scale Simulation of Runaway electrons on the Sunway TaihuLight Supercomputer

Based on APT-SW, the long-term evolution of runaway beam is simulated under parameters of ITER tokamak on the Sunway TaihuLight supercomputer. The background field is given by Eqs.14-15. In this simulation, the magnetic ripple field due to the finite toroidal coils is considered, which is modeled by [39, 71]

$$\delta\mathbf{B} = \delta B \mathbf{e}_r, \quad (17)$$

$$\delta B(r, \theta, \varphi) = \sum_{m=0, n=1}^{m=\infty, n=\infty} \delta B_{mn}(r) \cos(m\theta) \cos(nN\varphi), \quad (18)$$

where, r , θ , and φ are the components of toroidal coordinate, and N is the number of toroidal coils. Following the discussion by Laurent [71], we consider only the largest components of the series, *i.e.*, $m = 0, 1$. The radial profile of magnetic ripple amplitude is approximated by [72]

$$\delta B_{0n}(r) = \delta B_{1n}(r) \approx \eta_n B_0 \frac{r^2}{a^2}, \quad (19)$$

where, η_n are constants denoting the ratio of strength of n th order ripple to 0th order magnetic strength. Following the design of ITER [73, 74], the tokamak parameters are set as, $B_0 = 5$ T, $q = 2.5$, $R_0 = 6.2$ m, $a = 2$ m, $N = 18$, and $E_l = 4$ V/m. We consider the first three harmonics of magnetic ripple. For $n = 1$ harmonic, η_1 is set as 1% as in Ref. [74]. For $n = 2$ and $n = 3$ harmonics, the ratios are given by $\eta_2 = 0.2\%$ and $\eta_3 = 0.06\%$.

The initial poloidal profile of runaway beam is sampled based on a parabolic distribution, namely,

$$N(R, z) = N_0 \left[1 - \frac{(R - R_0)^2 + z^2}{r_{max}^2} \right], \quad (20)$$

where $N_0 = 2.7 \times 10^6 \text{ m}^{-2}$ is the sampling density at $r = 0$, and $r_{max} = 1.6$ m. The initial toroidal angle, φ_0 , is sampled uniformly from 0 to 2π ; the initial energy of particles, γ_0 , is sampled based on a normal distribution with average value $\mu = 4.75$ MeV and standard deviation $\sigma = 0.25$ MeV; the initial value of pitch-angle, $p_{\perp 0}/p_0$, is uniformly sampled from 0 to 0.3, and the initial gyro-phase is sampled uniformly from 0 to 2π . The total number of particle samples is on the order of 10^7 , while the total iteration number is approximately 10^{11} .

Figure 6 depicts the evolution of pitch-angle scattering with and without the magnetic ripple field. Without magnetic ripple, the pitch-angle distribution is concentrated in a small interval after long-term evolution, see the red curves in Fig. 6a-c. The pitch-angles of all the particles are approximate 0.04, which implies that the initial momentum and position distributions have little impact on the momentum value at energy limit. However, once the magnetic ripple field

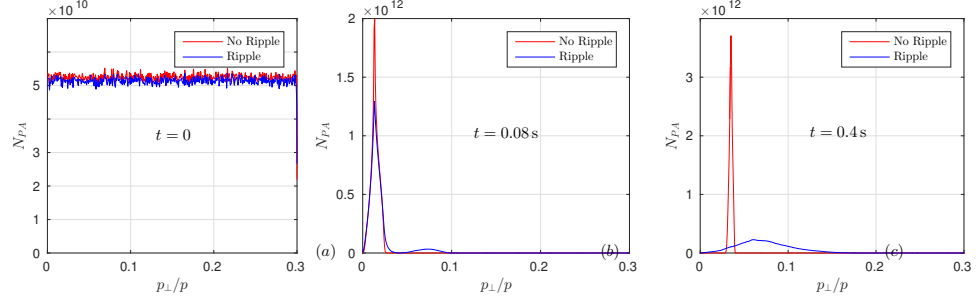


Figure 6: The pitch-angle distribution at different moments. The red curves show the results without magnetic ripple, while the blue curves are obtained after considering the magnetic ripple field.

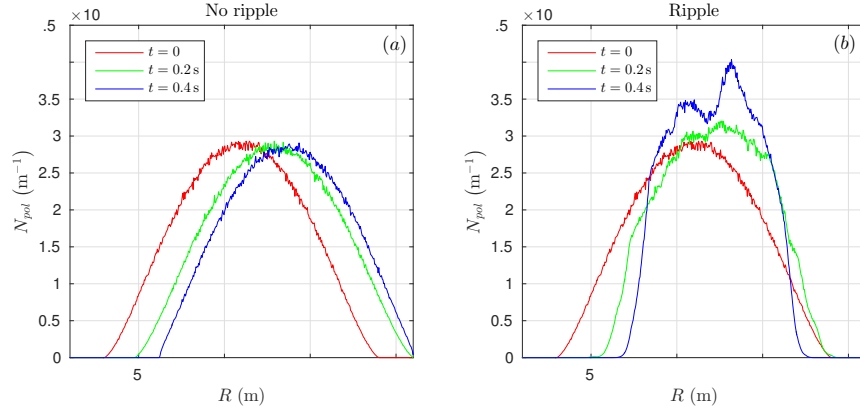


Figure 7: The poloidal profile of runaway beam at different moments. (a) shows the case without ripple field, and (b) depicts the result with magnetic ripple field. The magnetic ripple can concentrate the runaway profile near the core of tokamak.

is considered, even though the amplitude of perturbation is small, the evolution of pitch-angle distribution shows significant different behavior. To be specific, the pitch-angle distribution is broadened and the average value of perpendicular momentum gets larger.

Figure 7 shows the evolution of poloidal profile of runaway electrons. In the case without ripple field, the runaway profile drifts outward due to the neoclassical drift [14, 75], while the shape of the distribution keeps unchanged. Some electrons on the right-side hit the wall at $R = R_0 + a$. After considering magnetic ripple, the runaway beam is concentrated significantly near the core of tokamak, and no electron hits the first wall, which implies a better confinement of the runaways.

5. Conclusion

APT provides an efficient platform for large-scale particle simulations based on geometric algorithms. By tracing sampling particles, APT can reveal the microscopic and macroscopic dynamical behaviors of nonlinear and complex systems, such as magnetized plasmas, even in rather complex geometries. Without extra assumptions, the simulation model of APT is the first principle model, which obeys the characteristic line equations of the Vlasov-Maxwell system. The APT code consists of seven main modules, including the I/O module, the initialization module, the particle pusher module, the parallelization module, the field configuration module, the external force-field module, and the extendible module. The I/O module, supported by Lua and Hdf5 projects, provides a convenient and flexible interface for both numerical simulation and data analysis. Under the well-designed integrated and modularized framework, APT serves as a universal platform for researchers from different fields, such as plasma physics, accelerator physics, space science, fusion energy research, computational mathematics, software engineering, and high-performance computation.

In this paper, technical details of APT, including the numerical strategy, the parallelization techniques on different hardware architectures, and the in-

troductions for using and extending APT, are introduced. We exhibit the function interfaces of the containers for electromagnetic fields, external non-electromagnetic force fields, particle pushers, and initialization approaches. The three-step procedure of extending APT is provided, and the templates file of extendible functions are also shown. Following the instructions in Sec. 2.3, researchers with different backgrounds can use and extend the APT code conveniently.

A series of new geometric numerical methods and key physical problems, such as runaway electrons in tokamaks and energetic particles in Van Allen belt, have been studied using APT. The results reveal the long-term stability of APT. As an important realization, the APT-SW version has been successfully distributed on the world's fastest computer, the Sunway TaihuLight supercomputer, by supporting master-slave architecture of Sunway many-core processors. Based on large-scale simulations of runaway electrons under parameters of the ITER tokamak on the Sunway TaihuLight supercomputer, it is revealed that the magnetic ripple field can disperse the pitch-angle distribution significantly and improve the confinement of energetic runaway beam on the same time. The brand new physical results for solving complex multi-scale dynamical problems in fusion energy research exhibit the advantages of the APT code in long-term large-scale applications for complex realistic engineering problems.

In the next version, the algorithm evaluation module will be supplied in APT to evaluate the performance of numerical methods under different complex conditions. Based on this new module, the algorithm recommendation function can help users to find the optimum algorithm for a specific problem. The graphical user interface will also be developed to make APT more convenient to use. APT will also be equipped with more advanced geometric algorithms and applied to solve more pivotal scientific problems.

Acknowledgements

This research is supported by the CAS Key Program of Frontier Sciences

(QYZDB-SSW-SYS004), National Magnetic Confinement Fusion Energy Research Project (2015GB111003), National Natural Science Foundation of China (NSFC-11575185, 11575186), JSPS-NRF-NSFC A3 Foresight Program (NSFC-11261140328), and the GeoAlgorithmic Plasma Simulator (GAPS) Project.

References

References

- [1] A. Perona, D. Borgogno, L.-G. Eriksson, A test electron model for the study of three dimensional magnetic reconnection effects, *Comput. Phys. Commun.* 185 (1) (2014) 86.
- [2] B. Hamilton, L. Fletcher, K. McClements, A. Thyagaraja, Electron acceleration at reconnecting x-points in solar flares, *The Astrophysical Journal* 625 (1) (2005) 496.
- [3] D. Pfefferlé, W. Cooper, J. Graves, C. Misev, Venus-levis and its spline-fourier interpolation of 3d toroidal magnetic field representation for guiding-centre and full-orbit simulations of charged energetic particles, *Comput. Phys. Commun.* 185 (12) (2014) 3127.
- [4] R. White, M. Chance, Hamiltonian guiding center drift orbit calculation for plasmas of arbitrary cross section, *Phys. Fluids* 27 (10) (1984) 2455.
- [5] Z. Su, H. Zhu, F. Xiao, H. Zheng, M. Zhang, Y.-M. Liu, C. Shen, Y. Wang, S. Wang, Latitudinal dependence of nonlinear interaction between electromagnetic ion cyclotron wave and terrestrial ring current ions, *Phys. Plasmas* 21 (5) (2014) 052310.
- [6] S. Dalena, P. Chuychai, R. Mace, A. Greco, G. Qin, W. Matthaeus, Stream-line generation code for particle dynamics description in numerical models of turbulence, *Comput. Phys. Commun.* 183 (9) (2012) 1974.

- [7] R. C. Tautz, A new simulation code for particle diffusion in anisotropic, large-scale and turbulent magnetic fields, *Comput. Phys. Commun.* 181 (1) (2010) 71.
- [8] L.-G. Eriksson, P. Helander, Simulation of runaway electrons during tokamak disruptions, *Comput. Phys. Commun.* 154 (3) (2003) 175.
- [9] R. I. McLachlan, G. R. W. Quispel, Geometric integrators for odes, *J. Phys. A: Math. Gen.* 39 (19) (2006) 5251.
- [10] J. Candy, W. Rozmus, A symplectic integration algorithm for separable hamiltonian functions, *J. Comput. Phys.* 92 (1) (1991) 230.
- [11] H. Qin, X. Guan, Variational symplectic integrator for long-time simulations of the guiding-center motion of charged particles in general magnetic fields, *Phys. Rev. Lett.* 100 (3) (2008) 035006.
- [12] H. Qin, J. Liu, J. Xiao, R. Zhang, Y. He, Y. Wang, Y. Sun, J. W. Burby, L. Ellison, Y. Zhou, Canonical symplectic particle-in-cell method for long-term large-scale simulations of the vlasov-maxwell equations, *Nucl. Fusion* 56 (1) (2015) 014001.
- [13] H. Qin, S. Zhang, J. Xiao, J. Liu, Y. Sun, W. M. Tang, Why is boris algorithm so good?, *Phys. Plasmas* 20 (8) (2013) 084503.
- [14] X. Guan, H. Qin, N. J. Fisch, Phase-space dynamics of runaway electrons in tokamaks, *Phys. Plasmas* 17 (9) (2010) 092502.
- [15] R. Zhang, J. Liu, H. Qin, Y. Wang, Y. He, Y. Sun, Volume-preserving algorithm for secular relativistic dynamics of charged particles, *Phys. Plasmas* 22 (4) (2015) 044501.
- [16] J. Xiao, J. Liu, H. Qin, Z. Yu, A variational multi-symplectic particle-in-cell algorithm with smoothing functions for the vlasov-maxwell system, *Phys. Plasmas* 20 (10) (2013) 102517.

- [17] Y. He, H. Qin, Y. Sun, J. Xiao, R. Zhang, J. Liu, Hamiltonian time integrators for vlasov-maxwell equations, *Phys. Plasmas* 22 (12) (2015) 124503.
- [18] R. Zhang, J. Liu, Y. Tang, H. Qin, J. Xiao, B. Zhu, Canonicalization and symplectic simulation of the gyrocenter dynamics in time-independent magnetic fields, *Phys. Plasmas* 21 (3) (2014) 032504.
- [19] Y. He, Y. Sun, J. Liu, H. Qin, Higher order volume-preserving schemes for charged particle dynamics, *J. Comput. Phys.* 305 (2016) 172.
- [20] Y. He, Y. Sun, J. Liu, H. Qin, Volume-preserving algorithms for charged particle dynamics, *J. Comput. Phys.* 281 (2015) 135.
- [21] P. Channell, C. Scovel, Symplectic integration of hamiltonian systems, *Nonlinearity* 3 (2) (1990) 231.
- [22] P. J. Channell, Hybrid symplectic integrators for relativistic particles in electric and magnetic fields, *Comput. Sci. Discovery* 7 (1) (2014) 015001.
- [23] Y. He, Z. Zhou, Y. Sun, J. Liu, H. Qin, Explicit k-symplectic algorithms for charged particle dynamics, *Phys. Lett. A*.
- [24] J. Squire, H. Qin, W. M. Tang, Geometric integration of the vlasov-maxwell system with a variational particle-in-cell scheme, *Phys. Plasmas* 19 (8) (2012) 084501.
- [25] M. Kraus, O. Maj, Variational integrators for nonvariational partial differential equations, *Physica D* 310 (2015) 37.
- [26] M. Kraus, Variational integrators in plasma physics, *arXiv preprint arXiv:1307.5665*.
- [27] C. L. Ellison, J. Finn, H. Qin, W. M. Tang, Development of variational guiding center algorithms for parallel calculations in experimental magnetic equilibria, *Plasma Phys. Controlled Fusion* 57 (5) (2015) 054007.

- [28] J. Li, H. Qin, Z. Pu, L. Xie, S. Fu, Variational symplectic algorithm for guiding center dynamics in the inner magnetosphere, *Phys. Plasmas* 18 (5) (2011) 052902.
- [29] R. I. McLachlan, P. Atela, The accuracy of symplectic integrators, *Nonlinearity* 5 (2) (1992) 541.
- [30] B. Shadwick, A. Stamm, E. Evstatiev, Variational formulation of macroparticle plasma simulation algorithms, *Phys. Plasmas* 21 (5) (2014) 055708.
- [31] R. Zhang, H. Qin, Y. Tang, J. Liu, Y. He, J. Xiao, Explicit symplectic algorithms based on generating functions for charged particle dynamics, *Phys. Rev. E* 94 (1) (2016) 013205.
- [32] R. Zhang, Y. Wang, Y. He, J. Xiao, J. Liu, H. Qin, Y. Tang, Explicit symplectic algorithms based on generating functions for relativistic charged particle dynamics in time-dependent electromagnetic field, *arXiv preprint arXiv:1610.05390*.
- [33] B. Zhu, R. Zhang, Y. Tang, X. Tu, Y. Zhao, Splitting k-symplectic methods for non-canonical separable hamiltonian problems, *J. Comput. Phys.* 322 (2016) 387.
- [34] J. Xiao, J. Liu, H. Qin, Z. Yu, N. Xiang, Variational symplectic particle-in-cell simulation of nonlinear mode conversion from extraordinary waves to bernstein waves, *Phys. Plasmas* 22 (9) (2015) 092305.
- [35] M. Cadjan, M. Ivanov, Langevin approach to plasma kinetics with coulomb collisions, *J. Plasma Phys.* 61 (01) (1999) 89.
- [36] Top500 website, <https://www.top500.org/lists/2016/06/>.
- [37] H. Fu, J. Liao, J. Yang, L. Wang, Z. Song, X. Huang, C. Yang, W. Xue, F. Liu, F. e. a. Qiao, The sunway taihulight supercomputer: system and applications, *Science China Information Sciences* 59 (7) (2016) 072001.

- [38] J. Liu, Y. Wang, H. Qin, Collisionless pitch-angle scattering of runaway electrons, Nucl. Fusion 56 (6) (2016) 064002.
- [39] Y. Wang, H. Qin, J. Liu, Multi-scale full-orbit analysis on phase-space behavior of runaway electrons in tokamak fields with synchrotron radiation, Physics of Plasmas 23 (6).
- [40] J. Rax, N. Fisch, L. Laurent, Fast particle resonances in tokamaks, Plasma Phys. Contr. Fusion 35 (SB) (1993) B129.
- [41] Hdf5 website, <https://www.hdfgroup.org/HDF5/>.
- [42] Lua website, <https://www.lua.org/>.
- [43] E. Hairer, C. Lubich, G. Wanner, Geometric numerical integration: structure-preserving algorithms for ordinary differential equations, Vol. 31, Springer Science & Business Media, 2006.
- [44] H. Dreicer, Electron and ion runaway in a fully ionized gas. i, Phys. Rev. 115 (2) (1959) 238.
- [45] J. Connor, R. Hastie, Relativistic limitations on runaway electrons, Nucl. Fusion 15 (3) (1975) 415.
- [46] R. Yoshino, T. Kondoh, Y. Neyatani, K. Itami, Y. Kawano, N. Isei, Fast plasma shutdown by killer pellet injection in jt-60u with reduced heat flux on the divertor plate and avoiding runaway electron generation, Plasma Phys. Control. Fusion 39 (2) (1997) 313.
- [47] R. Jaspers, N. L. Cardozo, F. Schuller, K. Finken, T. Grewe, G. Mank, Disruption generated runaway electrons in textor and iter, Nucl. Fusion 36 (3) (1996) 367.
- [48] P. Helander, L.-G. Eriksson, F. Andersson, Suppression of runaway electron avalanches by radial diffusion, Phys. Plasmas 7 (10) (2000) 4106.

- [49] P. Helander, L. Eriksson, F. Andersson, Runaway acceleration during magnetic reconnection in tokamaks, *Plasma Phys. Contr. Fusion* 44 (12B) (2002) B247.
- [50] T. Fülöp, H. Smith, G. Pokol, Magnetic field threshold for runaway generation in tokamak disruptions, *Phys. Plasmas* 16 (2) (2009) 022502.
- [51] R. Gill, B. Alper, A. Edwards, L. Ingesson, M. Johnson, D. Ward, Direct observations of runaway electrons during disruptions in the jet tokamak, *Nucl. Fusion* 40 (2) (2000) 163.
- [52] R. Jaspers, K. Finken, G. Mank, F. Hoenen, J. Boedo, N. L. Cardozo, F. Schuller, Experimental investigation of runaway electron generation in textor, *Nucl. Fusion* 33 (12) (1993) 1775.
- [53] R. Nygren, T. Lutz, D. Walsh, G. Martin, M. Chatelier, T. Loarer, D. Guilhem, Runaway electron damage to the tore supra phase iii outboard pump limiter, *J. Nucl. Mater.* 241 (1997) 522.
- [54] P. Parks, M. Rosenbluth, S. Putvinski, Avalanche runaway growth rate from a momentum-space orbit analysis, *Phys. Plasmas* 6 (6) (1999) 2523.
- [55] M. Rosenbluth, S. Putvinski, Theory for avalanche of runaway electrons in tokamaks, *Nucl. Fusion* 37 (10) (1997) 1355.
- [56] R. Yoshino, S. Tokuda, Runaway electrons in magnetic turbulence and runaway current termination in tokamak discharges, *Nucl. Fusion* 40 (7) (2000) 1293.
- [57] H. Tamai, R. Yoshino, S. Tokuda, G. Kurita, Y. Neyatani, M. Bakhtiari, R. Khayrutdinov, V. Lukash, M. Rosenbluth, Runaway current termination in jt-60u, *Nucl. Fusion* 42 (3) (2002) 290.
- [58] M. Lehnen, S. Bozhnikov, S. Abdullaev, M. Jakubowski, Suppression of runaway electrons by resonant magnetic perturbations in textor disruptions, *Phys. Rev. Lett.* 100 (25) (2008) 255003.

- [59] K. Finken, S. Abdullaev, M. Jakubowski, R. Jaspers, M. Lehnen, R. Schlickeiser, K. Spatschek, A. Wingen, R. Wolf, Runaway losses in ergodized plasmas, *Nucl. Fusion* 47 (2) (2007) 91.
- [60] N. J. Fisch, Theory of current drive in plasmas, *Rev. Mod. Phys.* 59 (1) (1987) 175.
- [61] H.-W. Bartels, Impact of runaway electrons, *Fusion Eng. Des.* 23 (4) (1994) 323.
- [62] T. Kawamura, H. Obayashi, A. Miyahara, On the generation of runaway electrons and their impact to plasma facing components, *Fusion Eng. Des.* 9 (1989) 39.
- [63] H. Bolt, A. Miyahara, M. Miyake, T. Yamamoto, Simulation of tokamak runaway-electron events, *J. Nucl. Mater.* 151 (1) (1987) 48.
- [64] R. Jaspers, N. L. Cardozo, A. Donne, H. Widdershoven, K. Finken, A synchrotron radiation diagnostic to observe relativistic runaway electrons in a tokamak plasma, *Rev. Sci. Instrum.* 72 (1) (2001) 466.
- [65] J. Martín-Solís, J. Alvarez, R. Sánchez, B. Esposito, Momentum-space structure of relativistic runaway electrons, *Phys. Plasmas* 5 (6) (1998) 2370.
- [66] J. Martín-Solís, B. Esposito, R. Sánchez, J. Alvarez, Energy limits on runaway electrons in tokamak plasmas, *Phys. Plasmas* 6 (1) (1999) 238.
- [67] J. Liu, H. Qin, N. J. Fisch, Q. Teng, X. Wang, What is the fate of runaway positrons in tokamaks?, *Phys. Plasmas* 21 (6) (2014) 064503.
- [68] J. A. Van Allen, L. A. Frank, Radiation around the earth to a radial distance of 107,400 km, *Nature* 183.
- [69] Y. Chen, G. D. Reeves, R. H. Friedel, The energization of relativistic electrons in the outer van allen radiation belt, *Nat. Phys.* 3 (9) (2007) 614.

- [70] G. Reeves, H. E. Spence, M. Henderson, S. Morley, R. Friedel, H. Funsten, D. Baker, S. Kanekal, J. Blake, J. Fennell, Electron acceleration in the heart of the van allen radiation belts, *Science* 341 (6149) (2013) 991.
- [71] L. Laurent, J. Rax, Stochastic instability of runaway electrons in tokamaks, *Europhys. Lett.* 11 (3) (1990) 219.
- [72] A. Russo, Effect of ripple on runaway electrons in tokamaks, *Nuclear Fusion* 31 (1) (1991) 117.
- [73] R. Aymar, P. Barabaschi, Y. Shimomura, The iter design, *Plasma Phys. Controlled Fusion* 44 (5) (2002) 519.
- [74] A. Portone, M. Roccella, R. e. a. Roccella, The iter tf coil ripple: Evaluation of ripple attenuation using fe insert and of ripple enhancement produced by tbm, *Fusion Eng. Des.* 83 (10) (2008) 1619.
- [75] H. Qin, X. Guan, N. J. Fisch, Neoclassical drift of circulating orbits due to toroidal electric field in tokamaks, Report No. PPPL-4639, Princeton Plasma Physics Laboratory (PPPL), Princeton, NJ (United States) (2011).